



Published in final edited form as:

Lab Invest. 2015 October ; 95(10): 1145–1156. doi:10.1038/labinvest.2015.77.

Galectin 3 Regulates HCC cell invasion by RhoA and MLCK activation

Nobuko Serizawa¹, Jijiang Tian^{1,4}, Hiroo Fukada¹, Kornelia Baghy¹, Fiona Scott¹, Xiangling Chen¹, Zsofia Kiss¹, Kristin Olson², Dan Hsu³, Fu-Tong Liu³, Natalie J Török¹, Bin Zhao⁴, and Joy X. Jiang¹

¹Department of Internal Medicine, Division of Gastroenterology and Hepatology, UC Davis Medical Center, Sacramento, CA

²Department of Pathology, UC Davis Medical Center, Sacramento, CA

³Department of Dermatology, UC Davis Medical Center, Sacramento, CA

⁴State Key Laboratory of Environmental Chemistry and Ecotoxicology, Research Center for Eco-environmental Sciences, Chinese Academy of Sciences, Beijing, China

Abstract

Hepatocellular carcinoma (HCC) carries a poor prognosis with no effective treatment available other than liver transplantation for selected patients. Vascular invasion of HCC is one of the most important negative predictor of survival. As the regulation of invasion of HCC cells is not well understood, our aim was to study the mechanisms by which galectin 3, a β -galactosidase binding lectin mediates HCC cell migration. HCC was induced by N-diethylnitrosamine (DEN) in wild type and galectin 3^{-/-} mice, and tumor formation, histology, and tumor cell invasion were assessed. The galectin 3^{-/-} mice developed significantly smaller tumor burden with a less invasive phenotype than the wild type animals. Galectin 3 was upregulated in the wild type HCC tumor tissue, but not in the surrounding parenchyma. Galectin 3 expression in HCC was induced by NF- κ B transactivation as determined by chromatin immunoprecipitation assays. *In vitro* studies assessed the pro-migratory effects of galectin 3. The migration of hepatoma cells was significantly decreased after transfection by the galectin 3 siRNA and also after using the Rho kinase (ROCK) inhibitor Y-27632. The reorganization of the actin cytoskeleton, RhoA GTPase activity and the phosphorylation of MLC2 were decreased in the galectin 3 siRNA-transfected cells. In addition, *in vitro* and *in vivo* evidence showed that galectin 3 deficiency reduced hepatoma cell proliferation and increased their apoptosis rate. In conclusion, galectin 3 is an important lectin that is induced in HCC cells, and promotes hepatoma cell motility and invasion by an autocrine pathway. Targeting galectin 3 therefore could be an important novel treatment strategy to halt disease progression.

Users may view, print, copy, and download text and data-mine the content in such documents, for the purposes of academic research, subject always to the full Conditions of use:http://www.nature.com/authors/editorial_policies/license.html#terms

Address reprint to: Joy X. Jiang, M.D., Ph.D., UC Davis Medical Center, PSSB, 4150, V Street, Suite 3500, Sacramento, CA 95817. xiaosong.jiang@ucdmc.ucdavis.edu; fax: 916-734-7908, Phone: 916 734-0329.

Disclosure/Duality of Interest

The authors have no financial conflict or duality of interest to disclose.

Keywords

Galectin 3; hepatocellular carcinoma; cell migration; RhoA; MLC2

Hepatocellular carcinoma (HCC) is the third leading cause of cancer mortality worldwide (1), and its incidence and mortality rates continually rise. In the US it has the fastest growing death rate amongst all cancers (2). The only curative treatment approach is liver transplantation that is only available to the selected patients with localized early stage disease. HCC has a high metastatic and invasive potential leading to early recurrence after local ablative therapies or resection. The pathomechanism governing the invasiveness of HCC is poorly understood, and thus far there are no treatment strategies that can prevent HCC invasion. Galectin 3 is a unique 30 kDa molecule with a chimeric structure (3). As a member of the β -galactosidase binding lectin family, galectin 3 (also known as MAC-2) controls crucial cellular functions including cell adhesion, survival/apoptosis, regulation of adaptive immunity and macrophage activation (4–6). Galectin 3 also plays a role in the activation and transdifferentiation of hepatic stellate cells to myofibroblasts and in the progression of liver fibrosis (7,8). While normal hepatocytes do not express galectin 3, its expression was shown to be induced in patients with HCC (9,10), and in hepatocytes neighboring the fibrotic stroma in cirrhotic livers (9). In addition, tumor-associated macrophages in other tissues were also described as important sources of galectin 3 (11). In patients with HCC higher galectin 3 expression portended a worse overall survival (10). As the role of the galectin 3 in HCC progression has not been addressed, our goal was to assess the molecular mechanism by which galectin 3 contributes to tumor cell invasion. We have recently shown that galectin 3 binds to integrin $\alpha v \beta 3$ suggesting it play a role in ligand clustering on the cell surface, referred to as “galectin lattice” (12). As integrins can directly signal to Rho GTPases modulating the phosphorylation of the myosin light chain (MLC) we postulated that galectin 3 regulates the invasiveness of HCC cells by a RhoA/ROCK pathway (13). Herein we show that galectin 3 is induced by an NF κ B-dependent mechanism in HCC, and that galectin 3^{-/-} mice exhibit significantly smaller tumor burden after HCC induction with a less invasive phenotype. Galectin 3-induced RhoA/ROCK activation was required for the phosphorylation of the MLC2, leading to actin reorganization and migration of hepatoma cells. We conclude that galectin 3 is an important regulator of cell invasion during HCC progression.

Materials and Methods

Animals, and analysis of HCC Growth

Galectin3^{-/-} mice (kindly provided by Fu-Tong Liu, Department of Dermatology, UC Davis) in a C57/B6 background were generated by gene targeting technology, as described (14). As controls, age and sex-matched wild-type (wt) littermates were used. Male mice were injected by N-diethylnitrosamine (DEN) (5mg/kg, single dose ip. Sigma Aldrich, St. Louis, MO) at 4 weeks of age to induce HCC. Control mice were injected with the vehicle, only. The mice were then subjected for micro-CT scan and tissue harvest after 52 weeks. Tumor formation (size, location, number of satellite lesions) were assessed by micro-CT using Fenestra LC as a contrast agent (Inveon, Siemens Health Care Global, Erlangen,

Germany). The volumetric analysis was performed with the ASIPro VMsoftware (Concorde MicroSystems, Knoxville, TN).

Five wt and four galectin 3^{-/-} mice were included in this study. All procedures were reviewed and approved by the Animal Care Committee of the University of California Davis.

RNA interference

The immortalized mouse hepatoma cells Hepa1-6 (ATCC, Manassas, VA) were cultured in DMEM supplemented with 10% fetal bovine serum. The cells were maintained at 37°C in 5% CO₂ until the cells were 80% confluent, and then used for transfection.

SiRNA to galectin 3 (Santa Cruz Biotechnology, Santa Cruz, CA), or negative control scrambled siRNA (25nM, QIAGEN, Valencia, CA) was transfected into Hepa1-6 with RiboJuice transfection reagent (Novagen, Madison, WI), according to the manufacturer's instruction.

cDNA transfection

Hepa1-6 cells were transfected with the pCMX-IκBα phosphorylation mutant (kindly provided by S. Devaraj (Texas Children's Hospital, Houston, TX), originally from Addgene, pCMX-IκBα developed by Dr. Inder Verma (15), or the control vector (transfection efficiency, 60–70%), using the GeneJuice Transfection reagent (Novagen), following the manufacturer's instruction.

Chromatin immunoprecipitation and quantitative PCR (ChIP-qPCR) Assay

NFκB binding sites within mouse Gal3 promoter (+200 ~ -2000bp) were identified by PROMO online (<http://algggen.lsi.upc.es/cgi>). ChIP was carried out as described previously (16). After agarose gel electrophoresis and the product's size was confirmed with the average length 200–600 bp., rabbit anti-NFκB (p65) (Cell Signaling Technology, Beverly, MA) was used to pull down the transcription factor/DNA complex. Purified rabbit IgG (Santa Cruz Biotechnology Inc.) served as a control. Immunoprecipitated DNA was measured by qPCR for the respective NFκB binding sites using Power SYBR Green PCR master mix (Applied Biosystems, Foster City, CA). Primers were designed using Genscript online tool (<https://www.genscript.com/ssl-bin/app/primer>). A fragment (-205 to -137) adjacent to putative NFκB binding sites were amplified with primers: forward, 5'-GCAGGATGAGACCCTGACA-3', and reverse, 5'-GACCGCACCCAGACTCTC-3'. For qPCR results, the relative gene expression profile was achieved by normalizing the Ct of targets to the Ct of IgG ChIP of each sample. The data were presented as fold enrichment.

Wound closure assay

The scrambled or galectin 3 siRNA-transfected Hepa1-6 cells were incubated in the presence or the absence of recombinant galectin 3 (1μM, provided by Dr. F-T Liu, UC Davis). After 48 hours of transfection, the cultures were scraped with a single-edged razor blade. Twenty four hours later, five microscopic fields were evaluated, and the number of cells migrating across the wound edge were determined in each field and calculated for each

injury. In non-treated cells, migration was also assessed in the presence of Y-27632 (ROCK inhibitor, 10 μ M, Sigma, St Louis, MO). The experiments were repeated three times.

Immunohistochemistry and Immunofluorescence microscopy

The liver/tumor tissue was fixed in 4% buffered formalin and embedded in paraffin. H & E and reticulin staining were conducted by the department of pathology, UC Davis. The histology was analyzed by a hepatopathologist in a blinded fashion.

To detect galectin 3, the slides (4 μ m) were deparaffinized and rehydrated. For antigen retrieving, the slides were boiled in citrate buffer (0.01M, pH6.0). After incubated in 3% aqueous H₂O₂ to ablate endogenous peroxidase, the sections were washed in 0.1% Triton X-100 and blocked with the reagents provided by the UltraVision Protein Block (Thermo Scientific, Rockford, IL). Sections were then sequentially incubated with primary antibody (galectin 3, 1:1000, kindly provided by Dr. F-T Liu (17); glypican 3, 1:100, Abcam, Cambridge, MA), secondary HRP conjugated antibody (1:500, Santa Cruz Biotechnology, CA). The slides were then treated with DAB Substrates (Abcam) to visualize the signal and counterstained with Mayer's hematoxylin. The vascular invasion was quantified in 5 fields in each animal.

Human HCC sections were obtained from the department of pathology, UC Davis. Sequential sections were processed for DAB staining to detect galectin 3/glypican 3, and galectin 3/NF- κ B (p65) following the protocol described. NF- κ B (p65) antibody (1:200) was purchased from Cell signaling Technology.

Cryostat sections from the frozen liver/tumor tissue, in consecutive sections to those slides with H & E staining were co-stained with anti-galectin 3 and F4/80 antibodies (1:200, eBioscience, San Diego, CA) followed by fluorescence labeled secondary antibodies (Life Technology). The images were analyzed by fluorescent microscopy to assess the colocalization of galectin 3 and F4/80. The galectin 3⁺/F4/80⁺ cells were counted from 5 random views each slides. The cryostat sections were also probed with e-cadherin (1:500, BD Biosciences, San Jose, CA) to analyze the cell migratory activity. To assess the cell proliferation and apoptosis, Ki67 (Abcam) and active caspase-3 (1:500, Cell Signaling Technology) staining were performed. The positive cells in 5 fields were counted for each mouse.

To detect the cellular localization of RhoA, Hepa1-6 cells were transfected with scrambled or galectin 3 siRNA, fixed with 4% paraformaldehyde and permeabilized in 0.2% Triton X-100/PBS. After washing, they were blocked with 2% bovine serum albumin followed by incubating with anti-RhoA monoclonal antibody (1:40, Santa Cruz Biotechnology) for 16 hours at 4°C. The slides were then washed and incubated with rhodamine-conjugated phalloidin to visualize F-actin filaments. After washing, the secondary Alex Fluor 488-labeled anti-mouse IgG (1:1000, Life Technologies, Carlsbad, CA) was applied. The images were analyzed by fluorescence microscopy.

Hepa1-6 cells transfected with scrambled or galectin 3 siRNA were treated with fas ligand (5ng/ml, 16 hours, Millipore, Billerica, MA), and stained for active caspase 3. The cell proliferation was evaluated by Ki67 staining.

RNA extraction and real-time RT-PCR

RNA was extracted from the cells or tissues using RNeasy Mini kit (QIAGEN) following the manufacturer's instruction. cDNA was synthesized using the iScript cDNA Synthesis kit (Bio-Rad, Hercules, CA). The SYBR Green DNA Master mix (Applied Biosystems,) was used for real-time PCR analysis (Life Technologies). The galectin-3 primers used were described previously (8). For e-cadherin, the forward primer was 5'-CGAGAGAGTTACCCTACATA-3' and the reverse, 5'-GTGTTGGGGGCATCATCATC-3'; for vimentin, forward, 5'-GCACCCTGCAGTCATTCAGA-3' and reverse, 5'-CCACTTCCGTTCAAGGTCAAG-3'.

Rho activation, pull-down assay

Tumor tissue or siRNA-transfected Hepa1-6 cells were lysed and the supernatant was collected for the pull-down assay using a Rho activation assay kit (Millipore,). In brief, the cell lysates containing 1mg protein were mixed with glutathione-agarose beads bound with Rhotekin, containing a GTP-Rho binding domain. After incubation, the agarose beads were washed and collected by centrifugation, then resuspended in the sample buffer containing 1M dithiothreitol. The active GTP-Rho was released and denatured by boiling. The supernatant was collected and separated by SDS-polyacrylamide gel. The GTP-bound RhoA was detected by the antibody provided by the kit.

Western Blot analysis

Benign liver and tumor tissue was homogenized in RIPA buffer with protease inhibitor cocktails. The protein concentration was determined with the Bio-Rad protein assay kit (Thermo Scientific) and 20 µg of protein was separated by SDS-PAGE. The blot was probed with anti-galectin3 (kindly provided by Dr. F-T Liu, UC Davis) and anti-GAPDH (Trevigen, Gaithersburg, MD) as internal control. Hepa1-6 cells were transfected with scrambled or galectin3 siRNA, as above. Fifty µg of protein was used for Western blot. The blots were incubated with the appropriate antibodies for 16h at 4 C: anti-phospho-NFκB (p65) (Cell Signaling Technology), phospho MLC2 and MLC2 antibodies (Cell Signaling Technology), phospho-Akt and total Akt antibodies (Cell Signaling Technology) or the anti-galectin 3 antibody. The membranes were incubated with horseradish peroxidase-conjugated secondary antibodies (Santa Cruz Biotechnology) and the blots were developed by enhanced chemiluminescence (Thermo Scientific, Rockford, IL). The intensity of signals was quantified with ImageJ (National Institutes of Health, Bethesda, MD). The data were normalized to the expression of anti-GAPDH antibody.

Statistical Analysis

The data shown represent at least three experiments and expressed as the mean \pm SEM. Differences between groups were compared using one-way analysis of variance (ANOVA) associated with the Dunnett's test. Statistical significance was considered when $p < 0.05$.

Results

Galectin 3^{-/-} mice have a decreased tumor burden and a less invasive phenotype of HCC

To study the role of galectin 3 in an *in vivo* model of HCC, the wild type and galectin 3^{-/-} mice were injected with DEN or corn oil at the age of 4 weeks to induce HCC. Micro-CT scans were performed after 52 weeks to assess tumor size by volumetric analysis. (Fig. 1Aa–d). While in the wt mice the livers were largely replaced by tumors, the tumor burden in the galectin 3^{-/-} mice was significantly reduced (** $p < 0.01$, Fig. 1B). The liver tissues were harvested and processed for reticulin staining and glypican 3 immunohistochemistry staining to confirm the presence of HCC (Fig. 1C). Both wt and galectin 3^{-/-} mice remarkably lost reticulin stains in the tumor area (Fig. 1C a, b). They both were positive for another HCC marker glypican 3 (Fig. 1C c, d).

Based on the histological analysis (Fig. 2A), HCC from the wt mice exhibited more invasive properties with spindle-like cells and frequent vascular invasion (arrows). The tumors from the galectin 3^{-/-} mice exhibited a more differentiated, glandular phenotype, with histologically normal areas (nl) with portal tracts present. The vascular invasion foci were counted in five fields each animal (Fig. 2B). Significantly less vascular invasion was observed in the galectin 3^{-/-} livers. The mRNA levels of e-cadherin and vimentin were assessed to further evaluate the invasive properties in these tumor tissues (Fig. 2C, D). Wt tumors expressed significant lower level of e-cadherin (* $p < 0.05$) and higher level of vimentin, suggesting an invasive phenotype compared to the knockout tumors. The e-cadherin immunofluorescent staining also showed reduced e-cadherin in the wt tumor (Fig. 2E).

Fluorescent staining was also performed to detect Ki67 and active caspase 3 to assess the cell proliferation and apoptosis (Fig. 2F). The positive cells were quantified as described. The wt tumor showed higher proliferation activity and lower apoptosis.

Galectin 3 is upregulated in HCC tumor cells and tumor associated macrophages

Next we examined the expression of galectin 3 in HCC. Sequential sections from human HCC were stained with galectin 3 and HCC marker glypican 3 (Fig. 3A). The galectin 3 positive areas were highly identical with the glypican 3 positive areas, indicating the correlation of galectin 3 and HCC. In mice (Fig. 3B), galectin 3 was highly expressed in the DEN tumor, mainly in hepatoma cells; macrophages were positive as well (Fig. 3B, d, arrows). No galectin 3 signal was seen in normal hepatocytes (B, a). The induction of galectin 3 in HCC was then confirmed with Western blot analysis using benign and resected tumor tissues from the wt DEN mice (Fig. 3C, D). The expression of galectin 3 was significantly higher in tumors than that in the surrounding parenchyma (***) $p < 0.001$). As tumor associated macrophages were shown to express galectin 3, consecutive sections were

processed for H & E and immunofluorescent staining with galectin 3 and the macrophage marker F4/80 (Fig. 3F). Beside the increased galectin 3 expression in the tumor cells, there were a significantly higher number of macrophages co-expressing galectin 3 and F4/80 (Fig. 3F, G b–g, arrowhead) in the tumor tissues compared to the surrounding stroma (**p<0.01).

Galectin 3 induction in hepatoma cells is mediated by NF- κ B activation

To study the mechanism of galectin 3 upregulation in hepatoma cells, we focused on NF- κ B, as the induction of NF- κ B is a key event to the pathogenesis of HCC (18), and the promoter area of galectin 3 has been described to have NF- κ B-responsive elements (8,19,20). Sequential sections from human HCC were stained for galectin 3 and NF- κ B (p65) (Fig. 4A). The nuclear staining of p65 was observed in galectin 3 positive cells, suggesting the correlation of the activation of NF- κ B signaling and galectin 3 expression in HCC. Next, tumor tissues and adjacent benign tissue from DEN-treated WT mice were processed for CHIP-qPCR assay to assess the transcriptional regulation of NF- κ B on the galectin 3 promoter. The transactivation of NF- κ B within the mouse galectin 3 promoter was significantly induced in the tumor tissues (Fig. 4B, *p<0.05). To corroborate our *in vivo* data we transfected Hepa1-6 cells with the pCMX-I κ B α (phosphorylation mutant) vector to block the NF- κ B signaling cascade, or a control vector. The PCR data showed that the galectin 3 expression decreased in the pCMX-I κ B α -transfected cells (Fig. 4C, ***p<0.001), suggesting that NF- κ B plays an important role in galectin 3 induction in HCC carcinogenesis. To compare the activation of NF- κ B in wt and galectin 3^{-/-} tumors, the tissues were homogenized for Western blots to detect phospho-p65 (Fig. 4D, E). The phospho-65 level was significantly less in the knockout tumors (*p<0.05).

Galectin 3 induces the migration of HCC cells

Because of the observed histological differences, and the smaller tumor burden in the galectin 3^{-/-} mice we postulated that galectin 3 modulates the invasive properties of HCC cells. Hepa1-6 cells were transfected with scrambled or galectin 3 siRNA, and scratch assay was performed. The galectin 3 siRNA –transfected cells showed a significantly lower migratory activity compared to the cells transfected with scrambled siRNA (Fig. 4A and B, **p<0.01). The inhibition of migration was partially reversed by recombinant galectin 3 (Fig. 4A, d, and B, ***p<0.001), suggesting that extracellular galectin 3 is also involved in regulating HCC cell motility.

We also examined the proliferation and apoptosis rate of these cells (Fig. 5C–E). The hep1-6 cells expressing scrambled or galectin 3 siRNA were stained for Ki67. To evaluate the apoptosis, these cells were treated with fas ligand (FSL) prior the staining for active caspase 3. The Ki67⁺ cells were significantly reduced by galectin 3 siRNA (*p<0.05); and the active caspase 3⁺ cells were increased by galectin 3 silencing (**p<0.01). This confirmed our *in vivo* data that galectin 3 deficiency impaired cell proliferation and promoted apoptosis in mouse HCC (Fig. 2F).

As cytoskeletal remodeling is crucial in cell migration, next we focused on the galectin 3-mediated regulation and recruitment of the RhoA GTPase to the leading edge, and the reorganization of the actin cytoskeleton. Hepa1-6 cells were transfected with scrambled or

galectin 3 siRNA, and immunofluorescence microscopy was done to visualize F-actin filaments and RhoA (Fig. 6A). The galectin 3 siRNA-transfected cells exhibited different morphology with a more rounded phenotype, whereas the non-transfected or scrambled siRNA transfected cells had elongated, fusiform morphology. RhoA and F-actin were co-localized to the leading edge in the non-transfected and scrambled siRNA transfected cells (arrows). In contrast, these signals were cytoplasmic in the cells expressing the galectin 3 siRNA. To study RhoA activation, a pull-down assay was done to assess the GTP-bound RhoA in galectin 3 or scrambled siRNA-transfected cells. RhoA GTPase activation was decreased after transfection with the galectin 3 siRNA (Fig. 6B, C, * $p < 0.05$). The RhoA activation was also examined *in vivo*. The wt and the galectin 3^{-/-} tumor tissues were processed for the pull-down assay (Fig. 6D, E). The galectin 3^{-/-} tumors showed a lower level of active RhoA.

HCC cell migration is Rho-kinase and MLCK mediated

Because Rho kinase (ROCK) is a downstream effector of RhoA in the regulation of cytoskeletal reorganization and cell motility, Hepa1-6 cells were incubated with Y-27632 (ROCK inhibitor), and migration was assessed by a wound closure assay. The cell migration was significantly inhibited by Y-27632 (Fig. 7A and B, * $p < 0.05$). The contraction of the actin cytoskeleton through activation of myosin 2 is essential in exerting force to induce the cells motility (21). The actin-myosin 2 interaction is regulated by the phosphorylation of MLC2 on Ser-19 (22). The regulatory light chains of the myosin 2 (MLC2) are known to be phosphorylated by the myosin light chain kinase (MLCK) as a downstream target of ROCK (22). We found that in the galectin 3 siRNA-transfected Hepa1-6 cells, corresponding to the decrease in RhoA and ROCK activity; the phosphorylation of MLC2 was significantly reduced (Fig. 7C, D, * $p < 0.05$).

Discussion

Tumor cell migration and locoregional invasion are characteristic features of HCC spread, and because of the lack of satisfactory treatment options, these histological findings herald a poor prognosis. Because the remodeling of the cytoskeleton is crucial in cell migration, and the Rho family of small GTPases are known to regulate the actin cytoskeleton, (23,24) we have postulated that galectin 3 regulates and enhances RhoA activity in HCC tumor cells. Galectin 3 has been described to trigger signaling cascades by crosslinking with the glycan parts of the glycoconjugates (25), and we and others have shown that by binding to integrins it could elicit downstream signals affecting cytoskeletal reorganization and phagocytosis in hepatic stellate cells (8,12). In the current study we sought to understand the mechanism by which galectin 3 controls tumor cell motility. We found that RhoA GTPase activation and downstream ROCK and MLC2 phosphorylation leading to actin reorganization were dependent on galectin 3. RhoA/ROCK activation were described earlier as correlating to the locoregional invasion of human HCC (26), however the upstream regulators or cellular targets have not been fully evaluated. Discovering galectin 3 as a proximal inducer of the RhoA/ROCK pathway therefore could lead to novel therapeutic strategies. Targeting galectin 3 production or interfering with its ability to bind to the lattice could result in a less invasive phenotype, and a prolonged survival (27,28).

Whether the intra- or extra-cellular galectin 3 has a more dominant role in regulating cell motility is also an important question. In this study we mainly focused on the mechanistic aspects by which intracellular galectin 3 modulates invasiveness. Our data suggest that galectin 3 affects tumor cell migration by an autocrine process, as we found that galectin 3 was significantly induced in HCC cells, and siRNA targeting decreased the migratory activity. Nevertheless our data also suggest that galectin 3 produced in a paracrine manner likely by tumor associated macrophages can stimulate hepatoma cell motility possibly by affecting galectin 3/integrin crosslinking. The dominant cell type corresponding to the major source of galectin 3 production in HCC could be further studied in the future in cell specific knockout mice.

We have also tested the role of galectin 3 *in vivo* in the DEN-induced HCC model. The results indicated a decreased tumor burden, number of intrahepatic metastases, and a more differentiated tumor phenotype with the lack of vascular invasion in the galectin 3^{-/-} mice. HCC tumor cells and tumor associated macrophages were both positive for galectin 3. A plausible explanation for this is the induction of NF-κB transactivation, as we have shown in HCC tumor tissue and Hepa1-6 cells (Figure 4). NF-κB induction is an important step in HCC tumorigenesis (29–31), and its link to the increased HCC cell motility is well recognized (32,33). Galectin 3 induction of course can occur by other mechanisms as well, as it was shown that the epigenetic regulation of galectin 3 by β1 integrin induces cell motility (31). Galectin 3 can also be involved in other regulatory pathways in cancer cell migration. The expression level of galectin 3 in colon cancer cells is correlated with cell migratory activity and this is mediated by K-Ras/Raf/Erk signaling (34). Furthermore, as galectin 3 is a binding partner for β-catenin in immortalized breast cancer and colon cancer cells (35), it could be involved in the regulation of Wnt/β-catenin signaling cascade in HCC.

In addition our *in vitro* and *in vivo* data showed that galectin 3 deficiency in hepatoma cells is correlated with decreased proliferative activity and increased apoptosis (Figure 2F and Figure 5C). These are in an agreement to the previous findings that galectin 3 promotes cells proliferation and protect cells from proapoptotic stimuli (36,37).

Galectin 3 plays an important role in liver fibrosis by inducing the activation of hepatic stellate cells and promoting the deposition of the extracellular matrix (7,8). We have previously shown that the active myofibroblasts and Kupffer cells secrete galectin 3 (8). As the majority of HCCs arise in cirrhotic livers in humans, it is interesting to speculate that these cells beside tumor associated macrophages could also be important paracrine sources of galectin 3 in HCC tumorigenesis.

In summary, in this paper we have shown that galectin 3 promotes HCC cell migration, by inducing RhoA GTP-ase activity, MLC2 phosphorylation, and actin rearrangement required for a motile phenotype. *In vivo* galectin 3^{-/-} mice developed smaller tumor burden with a more differentiated phenotype in response to the carcinogen DEN. Development of therapeutic strategies targeting galectin 3 could prevent invasion and metastasis, and this in turn can lengthen a progression-free period that could bridge to liver transplantation.

Acknowledgments

We thank Dr. Simon Cherry and staff (Center for Molecular and Genomic Imaging, UC Davis) for micro CT scan; and Dr. Sridevi Devaraj (Texas Children's hospital) for providing the pCMX-I κ B α plasmid.

Abbreviations

HCC	hepatocellular carcinoma
NF-κB	nuclear factor kappa B
ROCK	Rho-associated protein kinase
MLC2	myosin light chain 2
DEN	N-diethylnitrosamine

References

1. Llovet JM, Burroughs A, Bruix J. Hepatocellular carcinoma. *Lancet*. 2003; 362:1907–1917. [PubMed: 14667750]
2. Altekruse SF, McGlynn KA, Reichman ME. Hepatocellular carcinoma incidence, mortality, and survival trends in the United States from 1975 to 2005. *J Clin Oncol*. 2009; 27:1485–1491. [PubMed: 19224838]
3. Liu FT. Molecular biology of IgE-binding protein, IgE-binding factors, and IgE receptors. *Crit Rev Immunol*. 1990; 10:289–306. [PubMed: 2150750]
4. Newlaczyl AU, Yu LG. Galectin-3--a jack-of-all-trades in cancer. *Cancer letters*. 2011; 313:123–128. [PubMed: 21974805]
5. Henderson NC, Sethi T. The regulation of inflammation by galectin-3. *Immunol Rev*. 2009; 230:160–171. [PubMed: 19594635]
6. MacKinnon AC, Farnworth SL, Hodgkinson PS, Henderson NC, Atkinson KM, Leffler H, Nilsson UJ, Haslett C, Forbes SJ, Sethi T. Regulation of alternative macrophage activation by galectin-3. *Journal of immunology*. 2008; 180:2650–2658.
7. Henderson NC, Mackinnon AC, Farnworth SL, Poirier F, Russo FP, Iredale JP, Haslett C, Simpson KJ, Sethi T. Galectin-3 regulates myofibroblast activation and hepatic fibrosis. *Proceedings of the National Academy of Sciences of the United States of America*. 2006; 103:5060–5065. [PubMed: 16549783]
8. Jiang JX, Chen X, Hsu DK, Baghy K, Serizawa N, Scott F, Takada Y, Fukada H, Chen J, Devaraj S, Adamson R, Liu FT, Torok NJ. Galectin-3 modulates phagocytosis-induced stellate cell activation and liver fibrosis in vivo. *Am J Physiol Gastrointest Liver Physiol*. 2012; 302:G439–446. [PubMed: 22159281]
9. Hsu DK, Dowling CA, Jeng KC, Chen JT, Yang RY, Liu FT. Galectin-3 expression is induced in cirrhotic liver and hepatocellular carcinoma. *International journal of cancer. Journal international du cancer*. 1999; 81:519–526. [PubMed: 10225438]
10. Matsuda Y, Yamagiwa Y, Fukushima K, Ueno Y, Shimosegawa T. Expression of galectin-3 involved in prognosis of patients with hepatocellular carcinoma. *Hepatol Res*. 2008; 38:1098–1111. [PubMed: 18684128]
11. Strik HM, Deininger MH, Frank B, Schluesener HJ, Meyermann R. Galectin-3: cellular distribution and correlation with WHO-grade in human gliomas. *Journal of neuro-oncology*. 2001; 53:13–20. [PubMed: 11678425]
12. Rabinovich GA, Toscano MA, Jackson SS, Vasta GR. Functions of cell surface galectin-glycoprotein lattices. *Curr Opin Struct Biol*. 2007; 17:513–520. [PubMed: 17950594]
13. Parri M, Chiarugi P. Rac and Rho GTPases in cancer cell motility control. *Cell communication and signaling: CCS*. 2010; 8:23. [PubMed: 20822528]

14. Hsu DK, Yang RY, Pan Z, Yu L, Salomon DR, Fung-Leung WP, Liu FT. Targeted disruption of the galectin-3 gene results in attenuated peritoneal inflammatory responses. *The American journal of pathology*. 2000; 156:1073–1083. [PubMed: 10702423]
15. Van Antwerp DJ, Martin SJ, Kafri T, Green DR, Verma IM. Suppression of TNF-alpha-induced apoptosis by NF-kappaB. *Science*. 1996; 274:787–789. [PubMed: 8864120]
16. Rubins NE, Friedman JR, Le PP, Zhang L, Brestelli J, Kaestner KH. Transcriptional networks in the liver: hepatocyte nuclear factor 6 function is largely independent of Foxa2. *Molecular and cellular biology*. 2005; 25:7069–7077. [PubMed: 16055718]
17. Liu FT, Hsu DK, Zuberi RI, Kuwabara I, Chi EY, Henderson WR Jr. Expression and function of galectin-3, a beta-galactoside-binding lectin, in human monocytes and macrophages. *The American journal of pathology*. 1995; 147:1016–1028. [PubMed: 7573347]
18. He G, Karin M. NF-kappaB and STAT3 - key players in liver inflammation and cancer. *Cell Res*. 2011; 21:159–168. [PubMed: 21187858]
19. Hsu DK, Hammes SR, Kuwabara I, Greene WC, Liu FT. Human T lymphotropic virus-I infection of human T lymphocytes induces expression of the beta-galactoside-binding lectin, galectin-3. *The American journal of pathology*. 1996; 148:1661–1670. [PubMed: 8623933]
20. Liu L, Sakai T, Sano N, Fukui K. Nucling mediates apoptosis by inhibiting expression of galectin-3 through interference with nuclear factor kappaB signalling. *Biochem J*. 2004; 380:31–41. [PubMed: 14961764]
21. Hakuma N, Kinoshita I, Shimizu Y, Yamazaki K, Yoshida K, Nishimura M, Dosaka-Akita H. E1AF/PEA3 activates the Rho/Rho-associated kinase pathway to increase the malignancy potential of non-small-cell lung cancer cells. *Cancer research*. 2005; 65:10776–10782. [PubMed: 16322223]
22. Matsumura F, Totsukawa G, Yamakita Y, Yamashiro S. Role of myosin light chain phosphorylation in the regulation of cytokinesis. *Cell Struct Funct*. 2001; 26:639–644. [PubMed: 11942620]
23. Caramel J, Quignon F, Delattre O. RhoA-dependent regulation of cell migration by the tumor suppressor hSNF5/INII. *Cancer research*. 2008; 68:6154–6161. [PubMed: 18676838]
24. Wong CC, Wong CM, Au SL, Ng IO. RhoGTPases and Rho-effectors in hepatocellular carcinoma metastasis: ROCK N'Rho move it. *Liver Int*. 30:642–656. [PubMed: 20726051]
25. Nangia-Makker P, Balan V, Raz A. Regulation of tumor progression by extracellular galectin-3. *Cancer Microenviron*. 2008; 1:43–51. [PubMed: 19308684]
26. Genda T, Sakamoto M, Ichida T, Asakura H, Kojiro M, Narumiya S, Hirohashi S. Cell motility mediated by rho and Rho-associated protein kinase plays a critical role in intrahepatic metastasis of human hepatocellular carcinoma. *Hepatology*. 1999; 30:1027–1036. [PubMed: 10498656]
27. Kahsai AW, Cui J, Kaniskan HU, Garner PP, Fenteany G. Analogs of tetrahydroisoquinoline natural products that inhibit cell migration and target galectin-3 outside of its carbohydrate-binding site. *The Journal of biological chemistry*. 2008; 283:24534–24545. [PubMed: 18556657]
28. Glinskii OV, Sud S, Mossine VV, Mawhinney TP, Anthony DC, Glinsky GV, Pienta KJ, Glinsky VV. Inhibition of prostate cancer bone metastasis by synthetic TF antigen mimic/galectin-3 inhibitor lactulose-L-leucine. *Neoplasia*. 2012; 14:65–73. [PubMed: 22355275]
29. Pikarsky E, Porat RM, Stein I, Abramovitch R, Amit S, Kasem S, Gutkovich-Pyest E, Urieli-Shoval S, Galun E, Ben-Neriah Y. NF-kappaB functions as a tumour promoter in inflammation-associated cancer. *Nature*. 2004; 431:461–466. [PubMed: 15329734]
30. Haybaeck J, Zeller N, Wolf MJ, Weber A, Wagner U, Kurrer MO, Bremer J, Iezzi G, Graf R, Clavien PA, Thimme R, Blum H, Nedospasov SA, Zatloukal K, Ramzan M, Ciesek S, Pietschmann T, Marche PN, Karin M, Kopf M, Browning JL, Aguzzi A, Heikenwalder M. A lymphotoxin-driven pathway to hepatocellular carcinoma. *Cancer cell*. 2009; 16:295–308. [PubMed: 19800575]
31. Margadant C, van den Bout I, van Boxtel AL, Thijssen VL, Sonnenberg A. Epigenetic Regulation of Galectin-3 Expression by beta1 Integrins Promotes Cell Adhesion and Migration. *The Journal of biological chemistry*. 2012; 287:44684–44693. [PubMed: 23118221]

32. Kastl L, Sauer SW, Ruppert T, Beissbarth T, Becker MS, Suss D, Krammer PH, Gulow K. TNF-alpha mediates mitochondrial uncoupling and enhances ROS-dependent cell migration via NF-kappaB activation in liver cells. *FEBS letters*. 2014; 588:175–183. [PubMed: 24316229]
33. Li J, Lau G, Chen L, Yuan YF, Huang J, Luk JM, Xie D, Guan XY. Interleukin 23 promotes hepatocellular carcinoma metastasis via NF-kappa B induced matrix metalloproteinase 9 expression. *PloS one*. 2012; 7:e46264. [PubMed: 23050001]
34. Wu KL, Huang EY, Jhu EW, Huang YH, Su WH, Chuang PC, Yang KD. Overexpression of galectin-3 enhances migration of colon cancer cells related to activation of the K-Ras-Raf-Erk1/2 pathway. *Journal of gastroenterology*. 2013; 48:350–359. [PubMed: 23015305]
35. Shimura T, Takenaka Y, Tsutsumi S, Hogan V, Kikuchi A, Raz A. Galectin-3, a novel binding partner of beta-catenin. *Cancer research*. 2004; 64:6363–6367. [PubMed: 15374939]
36. Inohara H, Akahani S, Raz A. Galectin-3 stimulates cell proliferation. *Experimental cell research*. 1998; 245:294–302. [PubMed: 9851870]
37. Hu Z, Jiang X, Xu Y, Lu N, Wang W, Luo J, Zou H, Zheng D, Feng X. Downregulation of galectin-3 by EGF mediates the apoptosis of HepG2 cells. *Molecular and cellular biochemistry*. 2012; 369:157–165. [PubMed: 22761016]

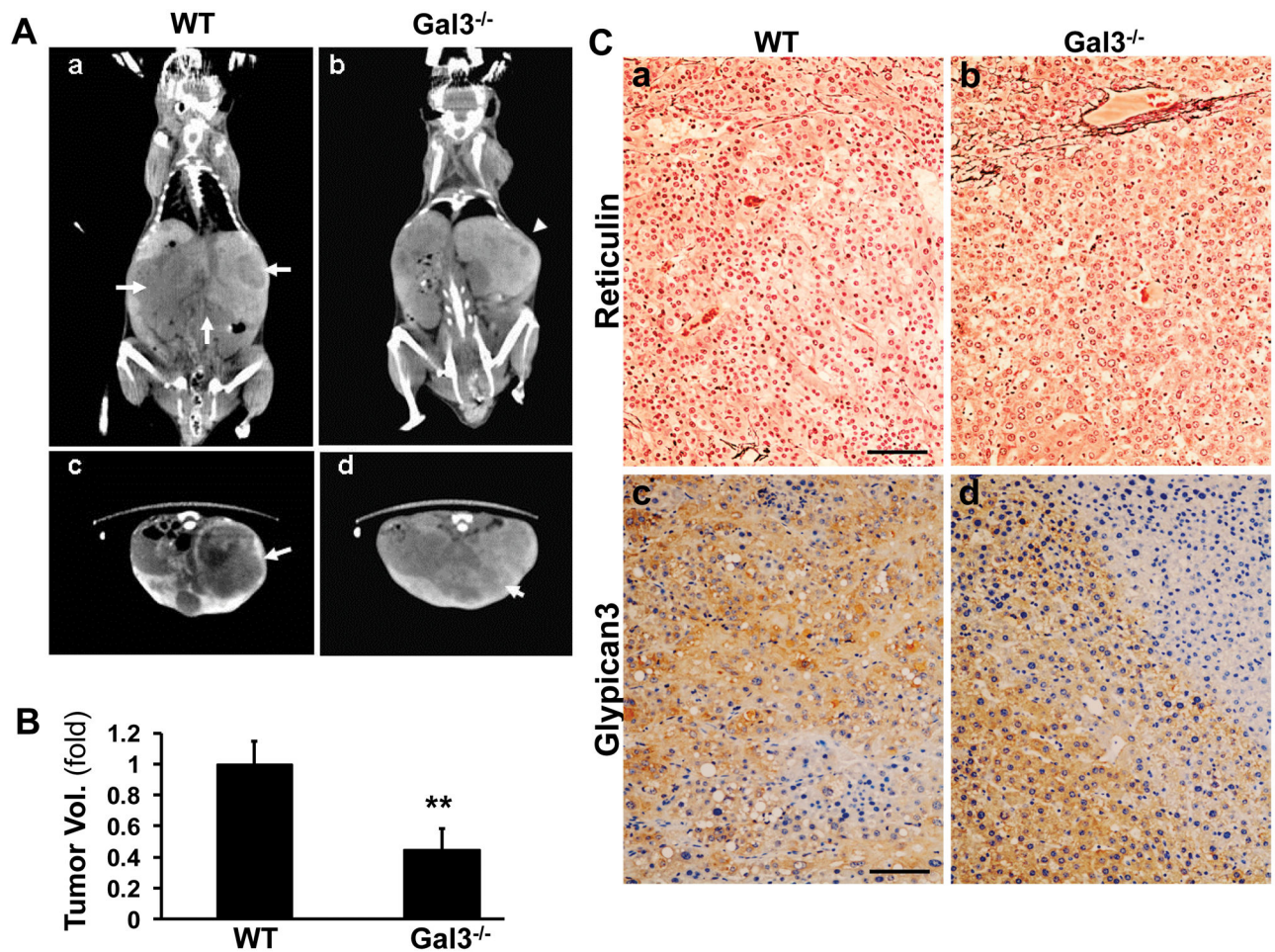
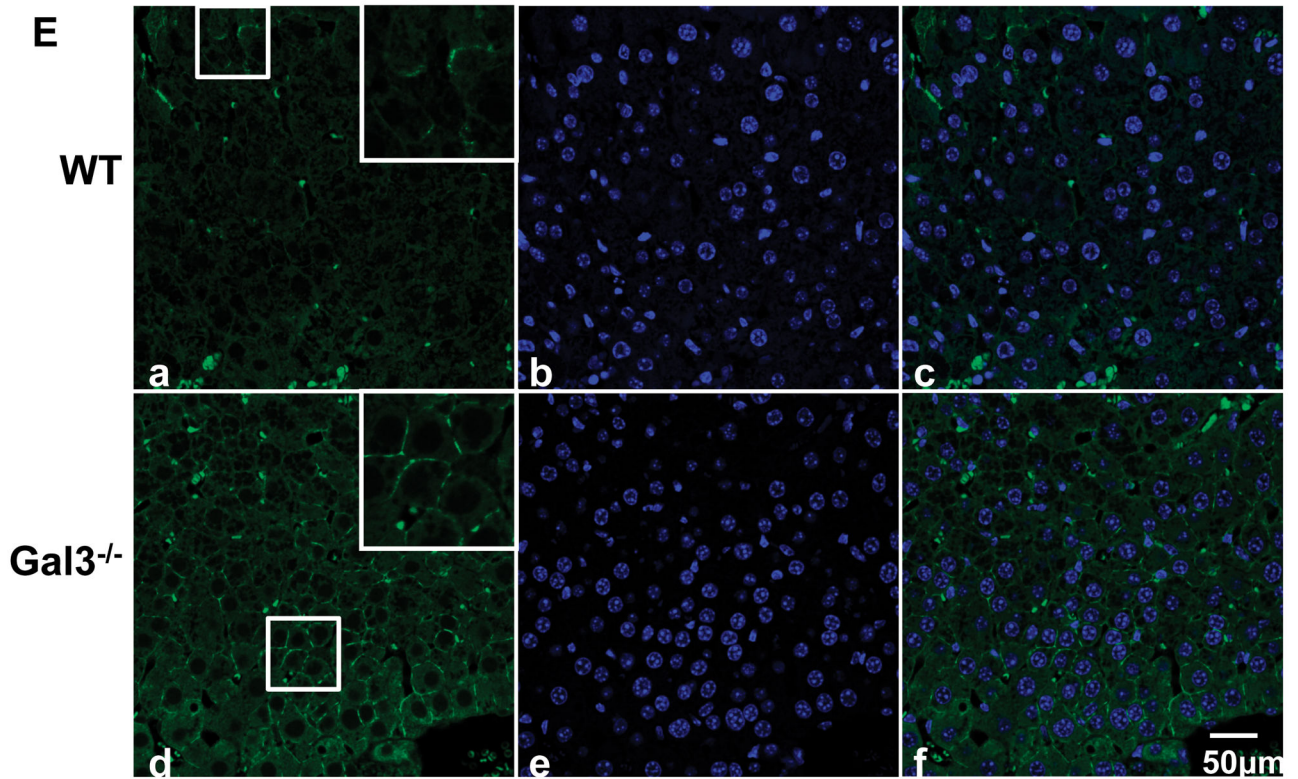
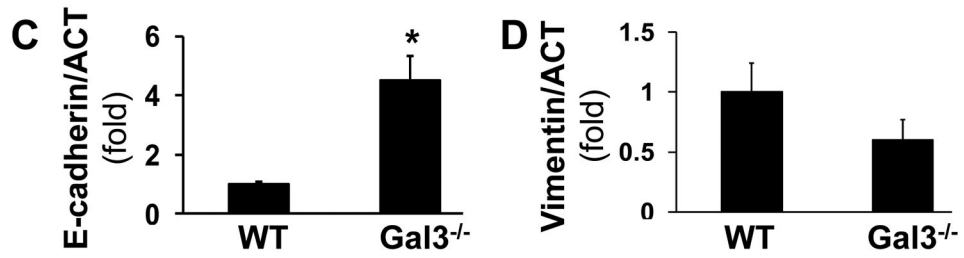
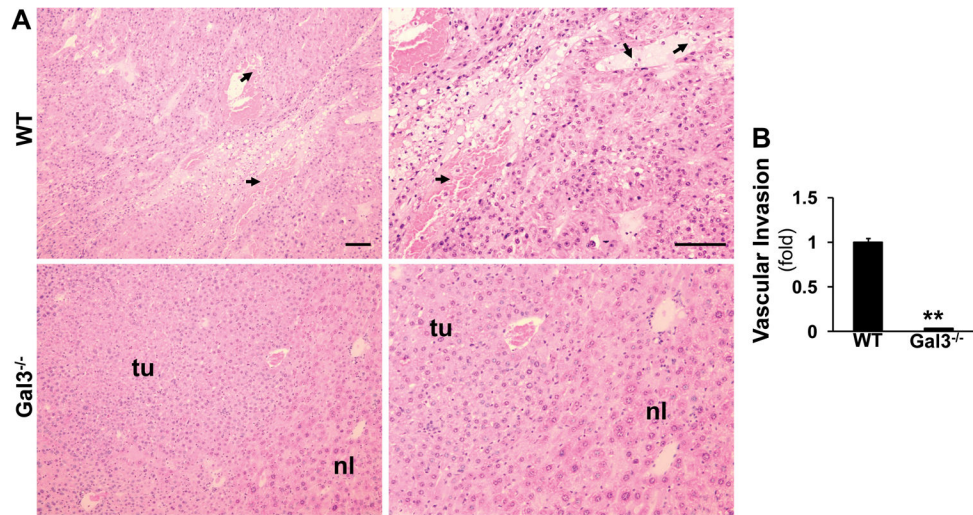


Figure 1. Galectin 3^{-/-} mice exhibit decreased tumor burden compared to the wild type mice
 Wild type and galectin 3^{-/-} mice were injected with DEN at 4 weeks of age to induce HCC. After 52 weeks, the mice were injected via tail vein with 200μl of the contrast agent Fenestra LC and subjected to Micro-CT scan. The tumor size was assessed by volumetric analysis (A). The HCC on the CT is depicted as large hypodense areas (arrows) in the wild type mouse, (coronal view, **a**; and horizontal view, **c**). In the galectin3^{-/-} mice smaller tumors were seen (**b** and **d**, arrowhead). By volumetric analysis, in the galectin 3^{-/-} mice the tumor burden was significantly lower. (B, **p<0.01, N=5). The liver tissues from these mice were processed for immunohistochemistry to detect reticulin (C, **a** and **b**) and glypican 3 (C, **c** and **d**). Both wt and galectin 3^{-/-} livers showed reduced reticulin and they were positive for glypican 3. This confirmed the presence of HCC in the mice. Bar=100 μm



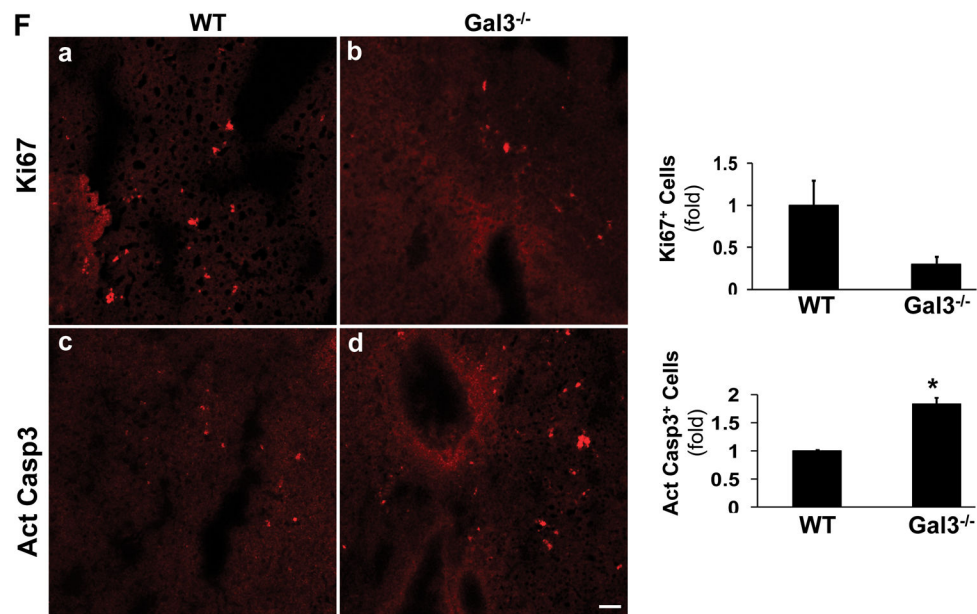


Figure 2. Galectin 3^{-/-} tumors show less invasive phenotype

Liver sections from the DEN-injected wild type and galectin 3^{-/-} mice were stained by H&E (A). HCC from the wild type (WT) mice exhibited more invasive properties with spindle-shaped cells whereas tumors from galectin3^{-/-} mice had a more differentiated phenotype (nl-normal, tu-tumor tissue. Vascular invasion was observed in WT tumors,(arrows). Bar=100 μ m. The foci of vascular invasion were counted in 5 fields from each animal (B).

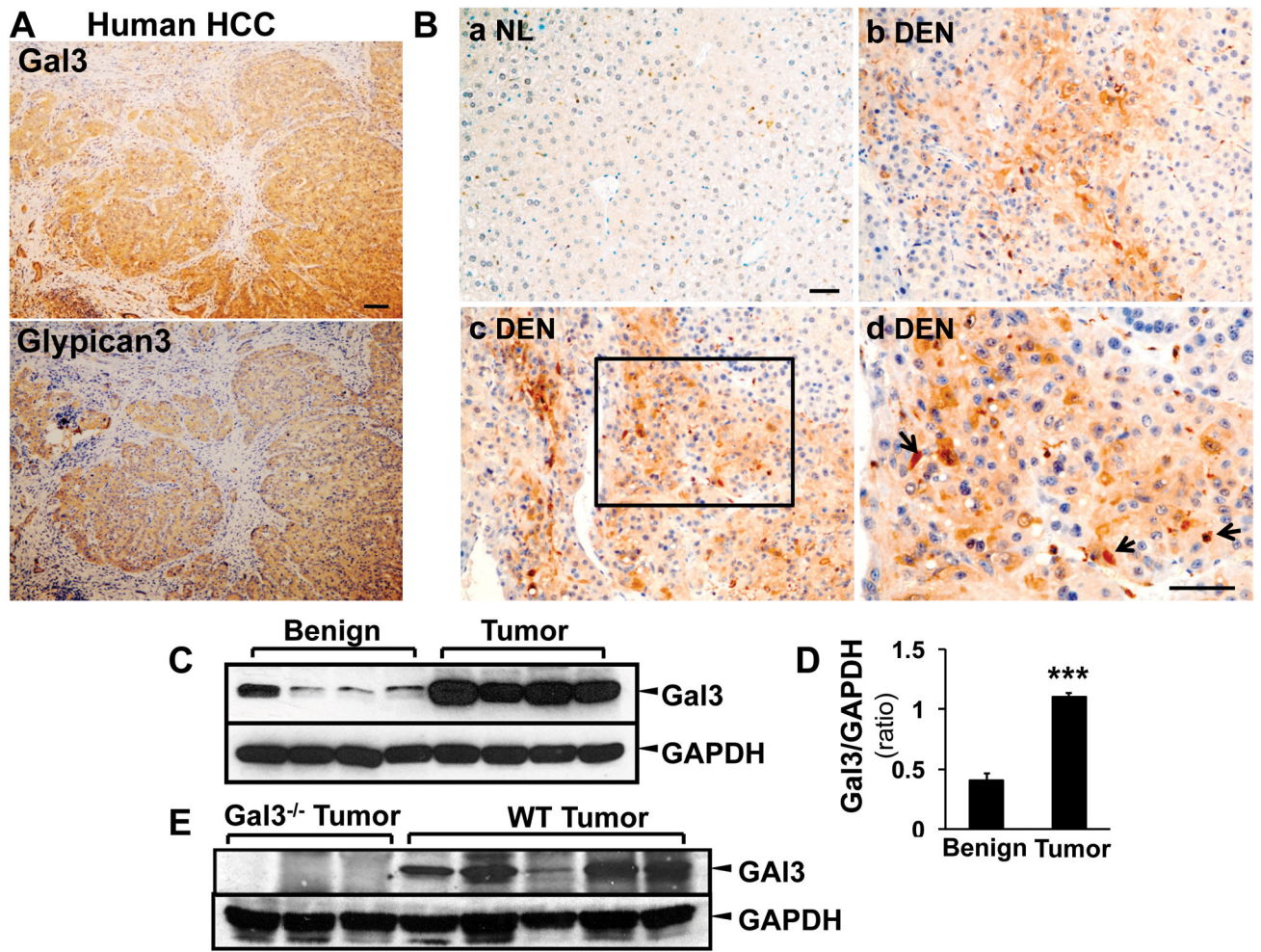
The wt mice showed significant more foci compared to the knockout mice (**p<0.01, N=4).

RT-PCR was conducted to measure the mRNA of e-cadherin and vimentin (C, D). The wt tumors expressed a significant higher level of e-cadherin (*p<0.05, N=4) and a lower level of vimentin, suggesting a high invasive phenotype compared to the galectin 3^{-/-} tumors.

Immunofluorescent staining was done on the frozen sections to detect e-cadherin (E).

Consistent with the PCR data, the wt tumor showed lower expression of e-cadherin. Bar=50 μ m.

The frozen sections were also stained for Ki67 and active caspase 3 (F). The positive cells were counted in 5 fields from each animal. The wt tumors showed more Ki67⁺ cells and less active caspase 3⁺ cells (*p<0.05).



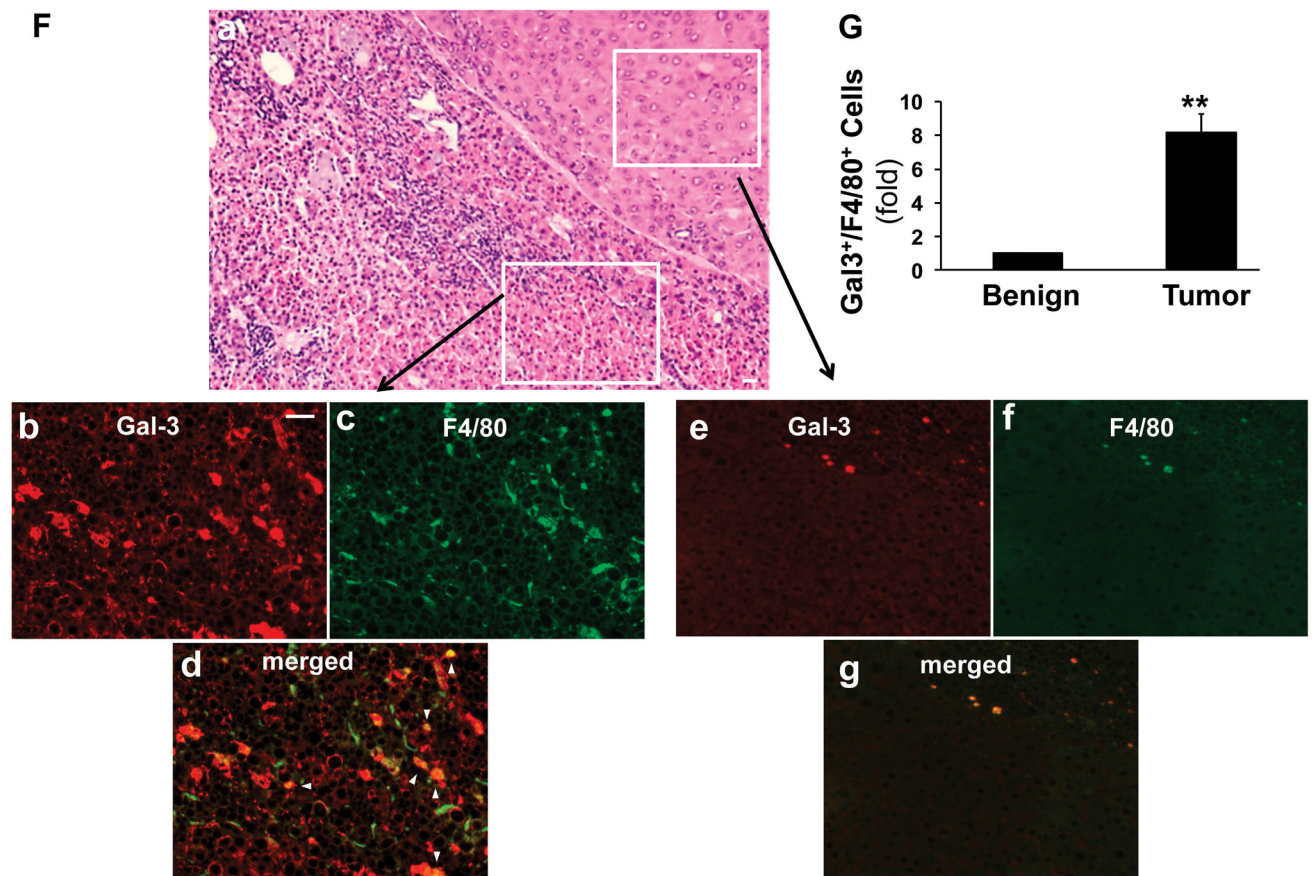


Figure 3. Galectin 3 is upregulated in HCC tumor cells and tumor associated macrophages
 Sequential sections from human HCC patients were used for immunohistochemistry staining targeting galectin 3 and glypican 3 (A). The image showed that the galectin 3 positive areas were highly identical with the glypican 3 positive areas in human HCC. The immunohistochemistry staining for galectin 3 was then conducted in the tissues from normal (NL) and wt DEN treated mice (B). Galectin 3 was highly expressed in DEN induced tumors (b–d), mainly in hepatoma cells. The high magnification image (B, d) depicted tumor-associated macrophages also expressing galectin 3 (arrow). Normal hepatocytes in control liver did not express galectin 3 (B, a). Western blot analysis and ImageJ quantification showed that galectin 3 expression was significantly higher in the tumor tissues (C, D, N=4, ***p<0.001). Western blot assay was also conducted on the wt and galectin 3^{-/-} tumors for antibody validation (E). No bands were detected in ~30kDa area in the knockout tumors and strong signals were shown in the wt tumors. Immunofluorescence and confocal microscopy on consecutive sections to the H&E-stained sections was performed to assess galectin 3 (red) and F4/80 (marker for tumor associated macrophages TAM, green, F). Analyzing the areas of HCC bordering the surrounding parenchyma, clusters of TAM co-expressed galectin 3 and F4/80 (b–d, arrowhead, Bar=50 μm) whereas no expression was seen in the normal hepatocytes and F4/80 positive cells were rare in the normal tissue (e–g). The tumor tissue carried a significant higher number of galectin 3⁺/F4/80⁺ cells (G, **p<0.01)

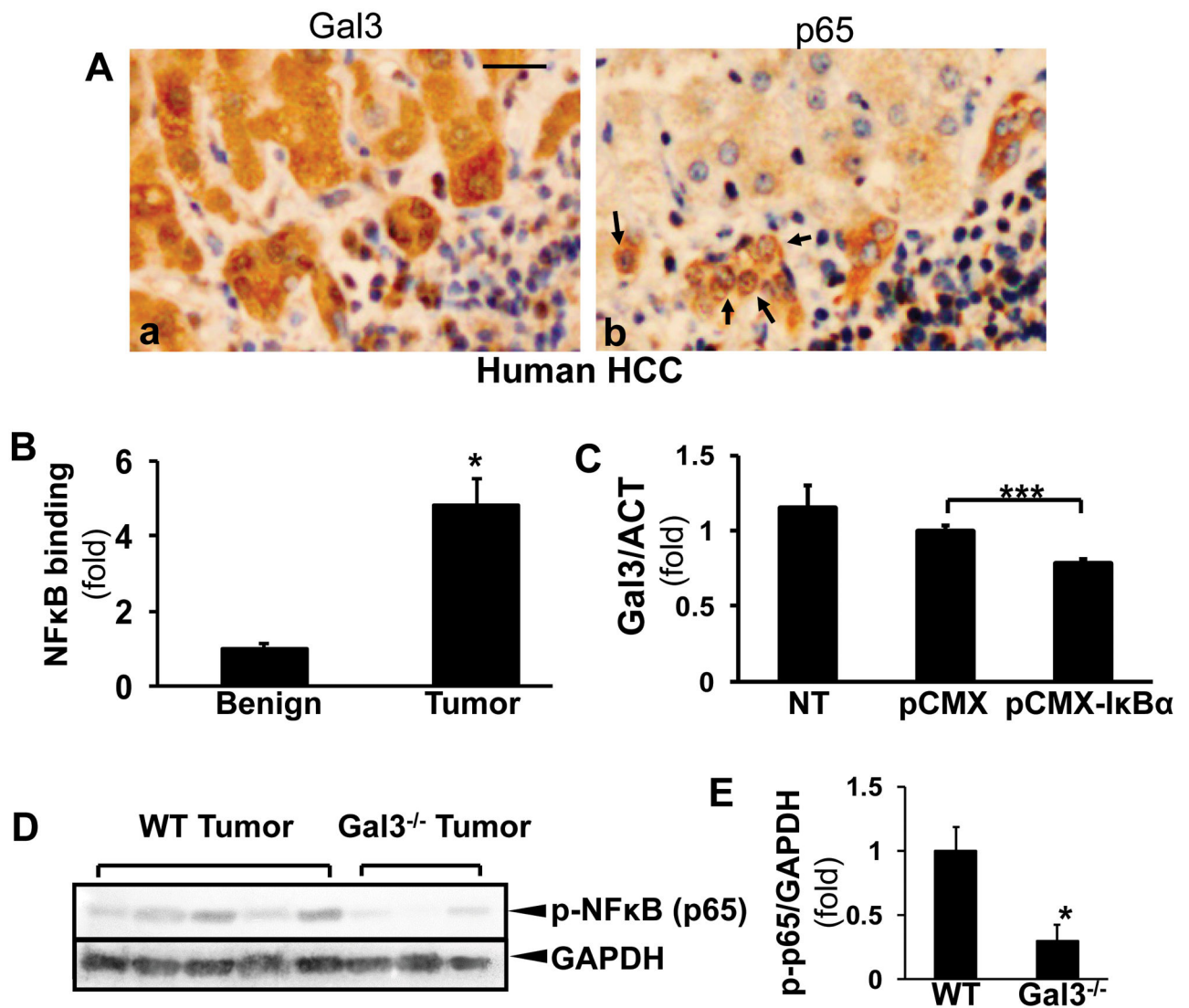


Figure 4. Galectin 3 expression in HCC is induced by NF-κB transactivation

Consecutive sections from human HCC were stained for galectin 3 and NF-κB (p65) (A).

The nuclear translocation (b, arrows) was observed in galectin 3 positive cells (Bar=50 μm).

ChIP assay was performed on benign tissue and DEN-induced tumors in WT mice (B). The NF-κB-induced transactivation of the Gal3 promoter was significantly induced in the tumor tissues compared to the benign controls (N=4, *p < 0.05).

Hepa1-6 cells were transfected with the pCMX-IκBα (phosphorylation mutant blocking the nuclear translocation of NF-κB) or the control vectors (C). RT-PCR showed that galectin 3 expression decreased in the pCMX-IκBα-expressing cells (mean±SEM, N=3, ***p<0.001).

The NF-κB phosphorylation was examined in wt and galectin 3^{-/-} tumors by Western blots (D, E) Less phospho-NF-κB was detected in the knockout tumors (*p<0.05).

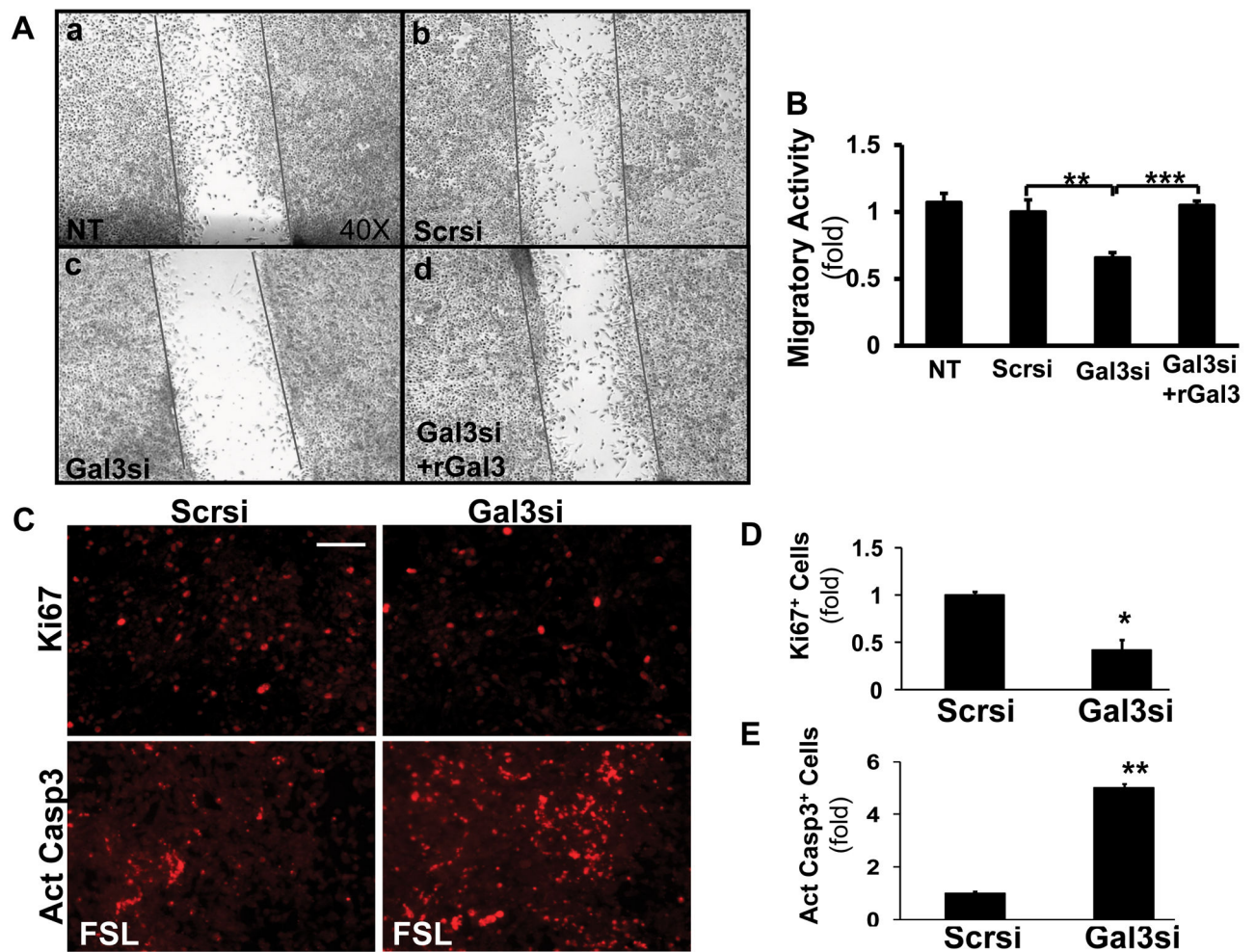


Figure 5. Galectin 3 mediates the migratory activity of hepatoma cells

To analyze the effect of galectin 3 on cell migration, Hepa1-6 cells were transfected with either scrambled (Scrsi) or galectin 3 siRNA (Gal3si), and 48 hours later wound closure assay was performed (A, B). Non-transfected (NT) cells were used as a control. After 24 hours, the number of migrating cells significantly decreased following galectin 3 siRNA transfection (N=9, **p<0.01) compared to the scrambled siRNA transfected cells. This was reversed by exposing the cells to recombinant galectin 3 (1 μ M for 24 hours), suggesting the role of extracellular galectin 3 in the regulation of HCC cell migration. (**p<0.01, ***p<0.001)

The above siRNA expressing cells were processed for fluorescent staining to detect Ki67 (C, D). The galectin 3 siRNA significantly reduced the number of Ki67⁺ cells (*p<0.05, N=4). To evaluate apoptosis, the above cells were incubated with fas ligand (FSL, 5 ng/ml, 16 hr), then stained for active caspase 3 (C, E). The galectin 3 siRNA significantly increased the number of active caspase 3⁺ cells (**p<0.01, N=4).

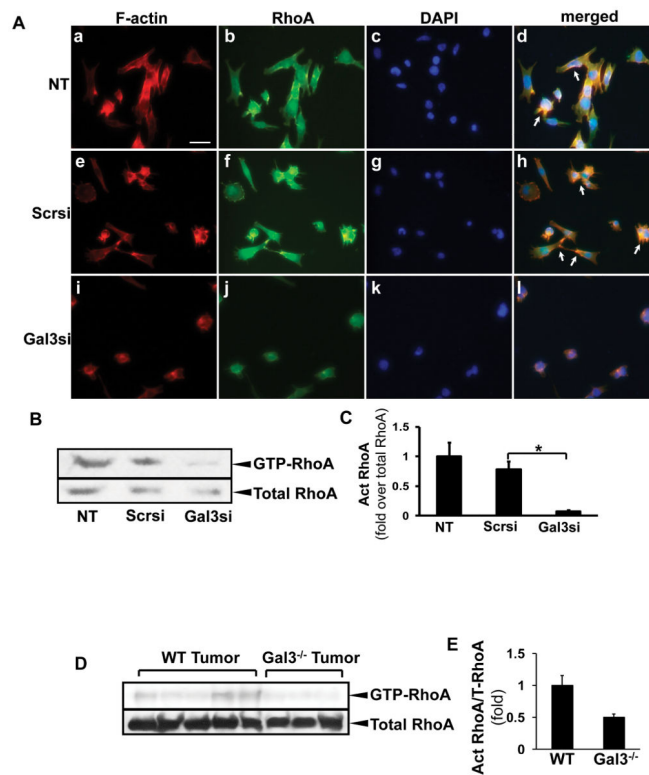


Figure 6. Galectin 3 inhibition results in the decrease in RhoA GTPase activity and actin reorganization in HCC cells

Hepa1-6 cells were transfected with either scrambled or galectin 3 siRNA. RhoA GTPase activity was assessed by pull-down of the GTP- RhoA in non-transfected (NT), scrambled or galectin 3 siRNA-transfected cells. RhoA activation was significantly decreased after galectin 3 siRNA transfection (**B, C**, mean±SEM, N=4, *p<0.05). The RhoA activation was examined in wt and galectin 3^{-/-} tumors as well (**D, E**). Less active RhoA was seen in the knockout tumors.

Immunofluorescence staining was performed to assess RhoA (**A: b, f, j**, green) localization and phalloidin (**A: a, e, i**, red) to visualize F-actin filaments. RhoA/F-actin was localized to the leading edges in the non-transfected (NT) and scrambled siRNA transfected cells (arrows). The galectin 3 siRNA-transfected cells had a more rounded shape with no lamellipodia formation and the RhoA staining was mainly cytoplasmic (Bar=20 μm).

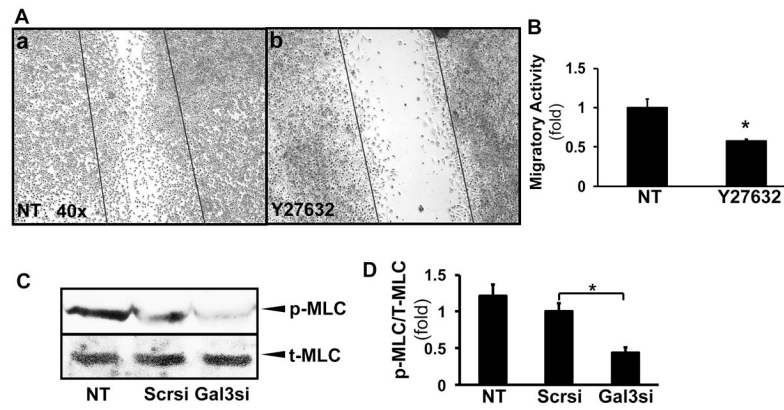


Figure 7. HCC cell migration is regulated by a ROCK and MLCK-mediated pathway resulting in MLC2 phosphorylation

Hepa1-6 cells were incubated with Y-27632 (ROCK inhibitor, 10 μ M), and a wound closure assay was performed. ROCK inhibition resulted in a significant decrease in the migratory rate compared to the control cells. (**A, B**; N=4, *p<0.05). The phosphorylation of MLC2 was examined as downstream target of galectin 3 and RhoA/ROCK by Western blots (**C**). Densitometry based on 3 independent experiments showed that in the galectin 3 siRNA-transfected cells, the phosphorylation of MLC2 was significantly reduced (**D**, N=3, *p<0.05).